

Journal of Materials Chemistry C

Accepted Manuscript



This is an *Accepted Manuscript*, which has been through the Royal Society of Chemistry peer review process and has been accepted for publication.

Accepted Manuscripts are published online shortly after acceptance, before technical editing, formatting and proof reading. Using this free service, authors can make their results available to the community, in citable form, before we publish the edited article. We will replace this *Accepted Manuscript* with the edited and formatted *Advance Article* as soon as it is available.

You can find more information about *Accepted Manuscripts* in the [Information for Authors](#).

Please note that technical editing may introduce minor changes to the text and/or graphics, which may alter content. The journal's standard [Terms & Conditions](#) and the [Ethical guidelines](#) still apply. In no event shall the Royal Society of Chemistry be held responsible for any errors or omissions in this *Accepted Manuscript* or any consequences arising from the use of any information it contains.



Journal Name

ARTICLE

Highly Efficient Emitters of Ultra-Deep-Blue Light Made from Chrysene Chromophores

Received 00th January 20xx,
Accepted 00th January 20xx

Hwangyu Shin,^a Hyocheol Jung,^a Beomjin Kim,^b Jaehyun Lee,^a Jiwon Moon,^a Joonghan Kim,^a and Jongwook Park^{*a}

DOI: 10.1039/x0xx00000x

www.rsc.org/

Chrysene, which has a wide band gap, was selected as an emission core to develop and study new materials that emit ultra-deep-blue light with high efficiency. Six compounds introducing various side groups were designed and synthesized: 6,12-Bis(3',5'-diphenylphenyl)chrysene (**TP-C-TP**), 6-(3',5'-diphenylphenyl)-12-(3''',5'''-diphenylbiphenyl-4''-yl)chrysene (**TP-C-TPB**) and 6,12-bis(3'',5''-diphenylbiphenyl-4''-yl)chrysene (**TPB-C-TPB**), which contained bulky aromatic side groups; and N,N,N',N'-tetraphenyl-chrysene-6,12-diamine (**DPA-C-DPA**), [12-(4-diphenylamino-phenyl)-chrysen-6-yl]-diphenylamine (**DPA-C-TPA**) and 6,12-bis[4-(diphenylamino)phenyl]chrysene (**TPA-C-TPA**), which contained aromatic amine groups and were designed to afford improved hole injection properties. The synthesized materials showed maximum absorption wavelengths at 342~402 nm in the film state and exhibited deep-blue photoluminescence (PL) emissions of 417~464 nm. Use of **TP-C-TPB** in a non-doped organic light-emitting diode (OLED) device resulted in ultra-deep-blue emission with an external quantum efficiency (EQE) of 4.02% and Commission Internationale de L'Eclairage coordinates (CIE x,y) of (0.154, 0.042) through effective control of internal conjugation length and suppression of π - π^* stacking. Use of **TPA-C-TPA**, which includes an aromatic amine side group, afforded an excellent EQE of 4.83% and excellent color coordinates of CIE x,y (0.147,0.077).

Introduction

Conjugated organic compounds that emit light have been examined in numerous studies due to their tunable optical and electronic properties, which make them candidate materials for applications such as displays and organic fluorescent sensors.¹ In particular, organic light emitting diodes (OLEDs) have been widely studied for their potential applications in full-color flat-panel displays, next-generation lighting and flexible displays.

Since electrons and holes are injected into the emitting layer and emission occurs from excitons formed inside OLEDs, the properties of the emitting materials are especially important for determining the efficiency and wavelength of OLEDs. Therefore, to achieve an effective full-color OLED display, it is essential to develop red, green and blue light-emitting materials that emit pure colors with high efficiency.² In the case of blue light-emitting materials for television displays in

particular, Commission Internationale de L'Eclairage coordinates (CIE x, y) of (0.14, 0.08) are required by the National Television System Committee (NTSC); and High-Definition Television (HDTV) ITU-R BT.709 requires a deeper blue emission of CIE x,y (0.15, 0.06).³ To date, however, the blue-emitting materials that meet these specifications have shown low efficiency. It is therefore necessary to develop a material that emits highly efficient deep-blue light. However, since a wide band gap, which is an intrinsic property of emitters of blue light, causes a relatively large energy level difference between adjacent hole- and electron-transporting layers, there has been considerable difficulty in developing materials that emit pure blue light with high efficiency.⁴ Conventional materials that emit blue light have mostly used anthracene,⁵ pyrene,⁶ and fluorene⁷ as core structures. However, while real blue and sky blue materials can be made with these core derivatives, it is difficult to achieve an emission of deep-blue light due to intrinsic limits on the conjugation length. Also, the rigid and planar structures of the molecules developed have led to broad and bathochromic emissions and to decreased emitting efficiency caused by intermolecular packing. Thus, it has been difficult to achieve a pure deep-blue wavelength with a CIE y value of 0.06 or below for blue light-emitting materials based on the core structures mentioned above.

Accordingly, in this study, to develop materials that emit deep-blue light with high efficiency, molecules were

^a Department of chemistry, Display Research Center, The Catholic University of Korea, Bucheon, 420-743, South Korea.
E-mail: hahapark@catholic.ac.kr

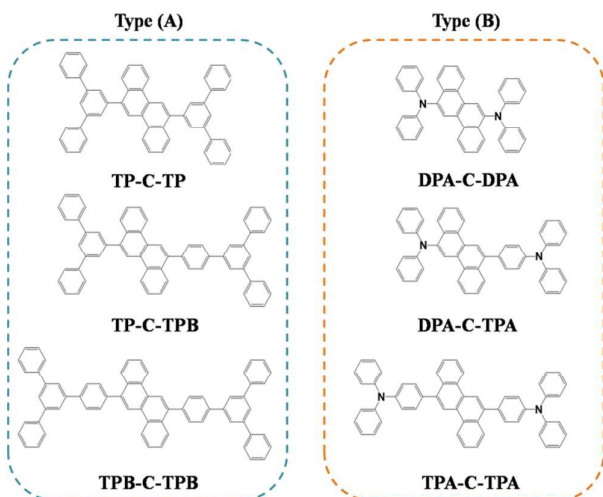
^b Department of chemistry, Research Center for Green Fine Chemicals, Korea Research Institute of Chemical Technology, Ulsan, 681-802, South Korea
†Electronic Supplementary Information (ESI) available: UV-vis absorption, PL and Normalized EL spectra. Synthetic routes. Dihedral angles. Absorption energies and oscillator strengths calculated using TD-CAM-B3LYP/6-311G(d,p) for synthesized compounds. See DOI: 10.1039/x0xx00000x

systematically designed and studied using the following three guides. 1) The key factor in studying emitters of deep-blue light is to select a core chromophore that controls intrinsic properties such as absorption and emission properties, thermal properties, and quantum efficiency. Also, deep-blue light can be made from the short conjugation length of organic emitter. The main core chromophore selected here was chrysene, which has a relatively short conjugation length. 2) Bulky aromatic rings were introduced as side groups to prevent broad and bathochromic emissions and to prevent decreases in the efficiency of chrysene core derivatives that might have otherwise occurred due to the planar structure of chrysene. 3) Aromatic amine groups were also tested as side groups to maintain the wide band gap intrinsic to materials that emit deep-blue light and to improve the hole-injection properties of the material.

The optical, thermal and electroluminescence properties of the materials made by following these guides were also studied. To our knowledge, this work is the first to use a chrysene chromophore as the core structure to develop organic materials that emit ultra-deep-blue light with high efficiency.

Results and Discussion

Molecular Design, Synthesis, and Optical Properties



Scheme 1. Chemical structures of synthesized emitting materials based on chrysene core chromophores.

Chrysene was introduced as the core because its ultraviolet-visible (UV-Vis) absorption maximum occurs in solution at a wavelength of 325 nm, which is shorter than those of anthracene and pyrene at 379 and 338 nm. (See Fig. S1[†]) This short wavelength is a result of the short intrinsic conjugation length and wide band gap of the chrysene core, which are appropriate for achieving deep-blue emission.

With regards to side groups, since substituting a side group into an electron-rich (lobe) position inside the core is more effective for adjusting molecular properties compared to

substitution into an electron-deficient (node) position,⁸ we substituted a variety of groups into these lobe positions. The lobe positions of chrysene are numbered 1, 4, 6, 7, 10, and 12, as shown in Fig. S2[†], and due to ease of synthesis, side groups were substituted into positions 6 and 12.

As shown in Scheme 1, bulky aromatic groups such as the *m*-terphenyl group and triphenylbenzene or aromatic amine groups such as diphenylamine and triphenylamine were symmetrically and asymmetrically substituted into positions 6 and 12 of chrysene, to prevent intermolecular packing or improve hole-injection properties. In 6,12-bis(3',5'-diphenylphenyl) chrysene (**TP-C-TP**), the *m*-terphenyl group was symmetrically substituted around the chrysene core; and in 6,12-bis(3'',5''-diphenylbiphenyl-4'-yl)chrysene (**TPB-C-TPB**), the triphenyl-benzene group was symmetrically substituted. 6-(3',5'-diphenylphenyl)-12-(3''',5'''-diphenylbiphenyl-4''-yl)chrysene (**TP-C-TPB**) is an asymmetric structure in which the *m*-terphenyl group and triphenylbenzene were substituted. Similarly, in N,N,N',N'-tetraphenyl-chrysene-6,12-diamine (**DPA-C-DPA**), the diphenylamine group was symmetrically substituted; and in 6,12-bis[4-(diphenylamino)phenyl]chrysene (**TPA-C-TPA**), the triphenylamine group was symmetrically substituted. Also, [12-(4-diphenylamino-phenyl)-chrysen-6-yl]-diphenylamine (**DPA-C-TPA**) is a molecule that was asymmetrically substituted with diphenylamine and triphenylamine.

The six synthesized materials were classified into type (A) for molecules whose bulky aromatic side group substituents consist only of a polyaromatic hydrocarbon and type (B) for molecules whose substituents include an aromatic amine side group, i.e., with a nitrogen heteroatom. The six compounds were synthesized through boronylation and Suzuki aryl-aryl coupling reactions as illustrated in Fig. S3[†], and the synthesized materials were characterized by nuclear magnetic resonance spectroscopy, elemental analysis, and Fast atom bombardment (FAB) mass analysis.

To determine the thermal properties of the synthesized molecules, thermal gravimetric analysis (TGA) and differential scanning calorimetry (DSC) were used, with the results summarized in Fig. S4 and Table 1. Molecules with high glass transition temperature (T_g) and decomposition temperature (T_d) values have an advantage in which morphology of the material is not easily changed by heat generated during operation of the OLED device.⁹ As shown in Table 1, the synthesized materials showed excellent thermal stability by exhibiting high T_d value of 360°C or above. Generally, increasing molecular weight results in an increase of the T_d value. In the case of T_g , **TP-C-TP**, **DPA-C-DPA** and **TPA-C-TPA** displayed high values of 177°C, 198°C and 253°C, respectively. These values are indicative of the excellent thermal properties compared to those of MADN, a well-known blue-light emitter containing an anthracene core and with a T_g of only 120°C. **TP-C-TPB** and **DPA-C-TPA** did not show T_m values. It might be due to the asymmetric molecular chemical structures.

The UV-Vis absorption spectra of the synthesized compounds are shown in Fig. 1 and summaries of these spectra are listed in Table 1. How the intramolecular electron density

distributions as well as the electronic transition origins of the various molecules differed from one another were calculated via density functional theory (DFT) calculations (CAM-B3LYP/6-311G(d,p)) to understand the differences between the optical properties of these molecules. The optimized molecular structures and their frontier molecular orbitals of the S_0 state molecular structures are shown in Fig. S5[†] and Fig. 2.

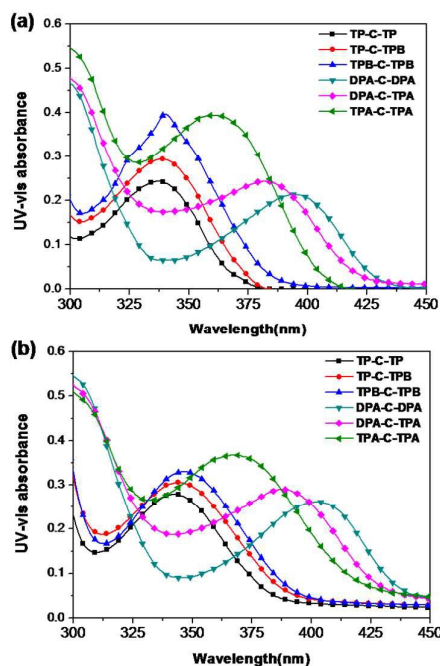


Fig 1. UV-vis absorption spectra of chrysene derivatives: (a) solution state, (b) film state.

In solution, the **TP-C-TP**, **TP-C-TPB** and **TPB-C-TPB** molecules, all type (A) and as described above characterized by bulky aromatic side groups, displayed maximum UV-Vis absorption wavelengths of 337, 338, and 340 nm, respectively, which are within 15 nm of the 325 nm intrinsic absorption wavelength of the chrysene core. This slight red shift may be due to the slightly expanded distribution of electron density to the substituents on the 6 and 12 positions of the core. Also, the triphenylbenzene side group of **TPB-C-TP** and **TPB-C-TPB**, having one more phenyl ring compared to the *m*-terphenyl side group of **TP-C-TP**, has a slightly increased conjugation length, helping to explain the 1~3 nm red shifts of the **TPB-C-TP** and **TPB-C-TPB** compounds compared to **TP-C-TP**. The UV-Vis absorption maximum wavelengths of **TP-C-TP**, **TPB-C-TPB** and **TPB-C-TPB** in the film state were observed to be, respectively, 342, 344 and 346 nm, showing a similar trend as in solution.

DPA-C-DPA, **DPA-C-TPA** and **TPA-C-TPA**, all type (B) molecules with aromatic amine side groups, displayed in the solution state maximum absorption wavelengths of 395, 382 and 361 nm, bathochromic shifts compared to the type (A) molecules. Unlike type (A) molecules, type (B) molecules showed a relatively wide distribution of the highest occupied

molecular orbital (HOMO) electron density throughout the diphenylamine and triphenylamine side groups instead of this density simply being limited to the chrysene core. For the lowest occupied molecular orbital (LUMO) of type (B) molecules, the distribution of electron density was focused on chrysene, unlike the HOMO shape, due to the electron-donating effect from the aromatic amine groups to the chrysene core.

These results indicate that introduction of aromatic amine side group affected the electron density and the HOMO level, and the change of HOMO level in turn led to a narrow band gap and bathochromic shift of the absorption wavelength. Also, **DPA-C-DPA**, whose core was substituted by two strongly electron-donating diphenylamine groups, showed maximum absorption at the longest wavelength of the compounds tested, i.e., at 395 nm. In contrast, **TPA-C-TPA**, with its two weakly electron-donating triphenylamine groups, showed maximum absorption in the 361 nm region. Note also that **DPA-C-DPA**, **DPA-C-TPA** and **TPA-C-TPA** in the film state yielded UV-Vis absorption maxima at, respectively, 402, 387 and 367 nm, a trend similar to the trend in solution.

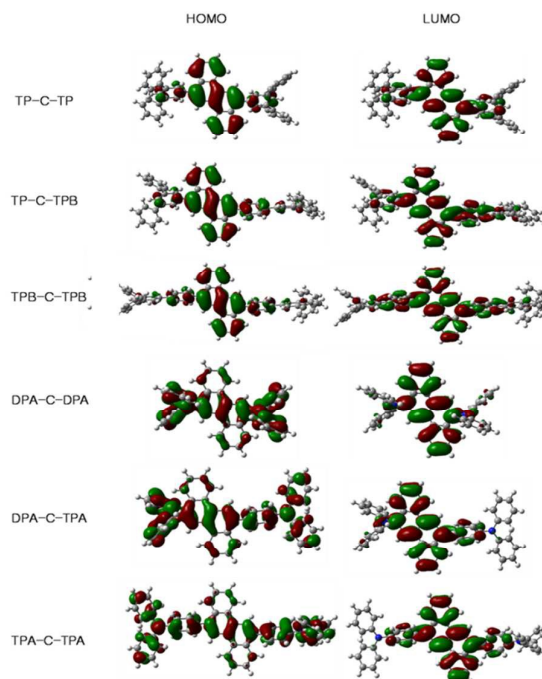


Fig 2. HOMO and LUMO electronic density distributions of the S_0 states of the compounds calculated at the CAM-B3LYP/6-311G(d,p) level.

HOMO, LUMO and band gap levels of the molecules are listed in Table 1 and were derived from the UV-Vis absorption spectroscopy in the film state and ultraviolet photoelectron spectroscopy (Riken-Keiki, AC-2). The HOMO and LUMO levels of the compounds with bulky aromatic side groups (i.e., type (A)) were determined to be in the range of -5.84 to -5.89 eV and -2.64 to -2.74 eV, respectively.

Table 1. Optical and thermal properties of synthesized compounds

Compound	Solution ^(a)			Film ^(b)			T_g	T_m	T_d	PL QY ^(c) (%)	HO MO (eV)	LU MO (eV)	Band gap (eV)
	UV (nm)	PL (nm)	FWHM (nm)	UV (nm)	PL (nm)	FWHM (nm)							
TP-C-TP	337	400	52	342	417	59	177	355	426	35	-5.88	-2.64	3.24
TP-C-TPB	338	407	56	344	425	49	-	-	463	53	-5.84	-2.66	3.18
TBP-C-TPB	340	415	58	346	433	55	-	361	504	48	-5.89	-2.74	3.15
DPA-C-DPA	395	455	50	402	464, 501	80	198	321	361	32	-5.49	-2.67	2.82
DPA-C-TPA	382	453	54	387	457	51	-	-	407	64	-5.53	-2.63	2.90
TPA-C-TPA	361	450	59	367	453	54	253	338	461	70	-5.51	-2.56	2.95

(a) 1×10^{-5} M in chloroform, (b) Film thickness is 50nm on the glass, (c) The solid-state absolute quantum yield on the quartz plate using an integrating sphere apparatus.

The band gap of **TP-C-TP** was found to be 3.24 eV, and the band gap of **TP-C-TPB** was slightly reduced to 3.18 eV due to the increased intramolecular conjugation length.

TPB-C-TPB yielded a further reduced band gap of 3.15 eV. The HOMO and LUMO levels of the molecules with aromatic amine side group (i.e., type (B)) were measured to be -5.49 to -5.53 eV and -2.56 to -2.67 eV, respectively. While these HOMO levels were found to be on average 0.36 eV greater than those of the type (A) molecules, because of the electron-donating side groups in the type (B) molecules, the LUMO values were not found to be significantly different between the type (B) and type (A) molecules. Of the tested type (B) molecules, **DPA-C-DPA**, with its strongly electron-donating side group, showed the narrowest band gap of 2.82 eV. However, as the side group was changed to triphenylamine, the band gap increased to 2.90 eV in **DPA-C-TPA** and 2.95 eV in **TPA-C-TPA**. This increase in band gap resulted from the reduced increase of the HOMO level upon changing the side group to triphenylamine, which has a weaker electron-donating effect on the core and is bulkier than diphenylamine. Accordingly, **TPA-C-TPA** showed the widest band gap among the type (B) materials.

Photoluminescence (PL) spectra of the synthesized compounds were obtained, and the data are shown in Fig. 3, Fig. S6[†] and Table 1. **TP-C-TP** showed a PL maximum (PL_{max}) value of 400 nm in the solution state and a PL_{max} of 417 nm in the film state. These emissions are in an extremely deep-blue wavelength region in comparison to those exhibited by anthracene (MAM, 439 nm) and pyrene (TP-Py-TP, 460 nm) cores symmetrically substituted by the *m*-terphenyl group as

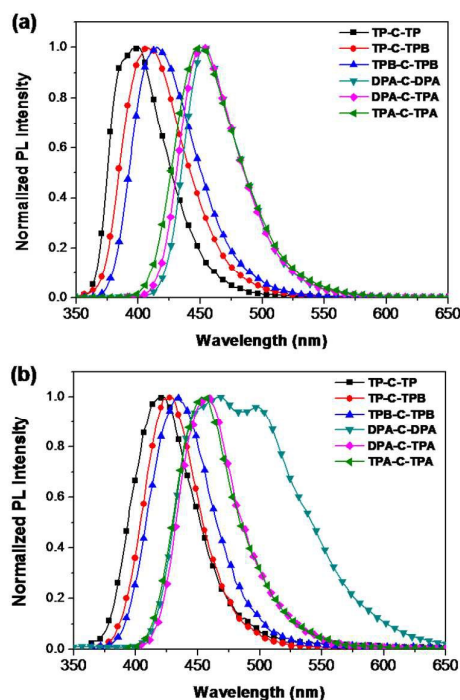


Fig 3. Normalized PL spectra of chrysene derivatives: (a) solution state, (b) film state.

reported previously (see Table S1[†]). **TP-C-TPB** and **TPB-C-TPB** displayed PL_{max} values of 407 and 415 nm in the solution state

and 425 and 433 nm in the film state. As observed for their UV-Vis absorption, the PL_{\max} values of these two molecules were slightly red-shifted compared to that of **TP-C-TP**, consistent with their increased intramolecular conjugation lengths, yet still with emissions at extremely short wavelengths of 430 nm or below.

The type (B) molecules, i.e., those substituted by aromatic amine moieties, showed longer emission wavelengths than did the type (A) molecules, because of the electron-donating aromatic amine group. **DPA-C-DPA** displayed the longest PL_{\max} wavelength, at 455 nm, of the molecules tested in the solution state. The PL_{\max} of **DPA-C-TPA** was 453 nm, and that of **TPA-C-TPA**, with its triphenylamine side groups, was slightly blue shifted to 450 nm. An identical trend was observed in the film state. But **DPA-C-DPA**, unlike the other molecules, displayed a broad emission spectrum in the film state with two PL_{\max} values, at 464 nm, 501 nm and shoulder emission peak at 540 nm. This feature was probably caused by a solid-state-specific intermolecular excimer, resulting from the relatively small size of the diphenylamine side group. 464, 501 and 540 nm emission peaks were observed from **DPA-C-DPA** using time-resolved fluorescence spectroscopy in the film state. (see Fig. S7(a)†). Also, to clarify whether the emission at 501 and 540 nm are an excimer peaks corresponding to PL emission from the molecule, excitation spectra were measured along with the UV-vis absorption spectrum (see Fig. S7(b)†). The UV-vis absorption spectrum matched well with the excitation spectra. The excitation spectra monitored at 464, 501 and 540 nm are very similar, indicating that they arise from the same excitation pathway. These findings are consistent with the 501 and 540 nm peaks being an excimer emission.

Previously studied anthracene and pyrene core derivatives showed emission wavelength shifts to the green region when an aromatic amine moiety was directly substituted into the emission core.¹⁰ But in our type (B) chrysene core materials, the emission was shown in the deep blue region, at 450 nm or below despite the substitution of the aromatic amine moiety. Since the chrysene core offers a large band gap, it can still emit deep-blue light even when the band gap is somewhat reduced by the introduction of the electron-donating side group.

The full widths at half maximum (FWHMs) of the solution PL spectra of **TP-C-TP**, **TP-C-TPB** and **TPB-C-TPB** were measured to be 52 nm, 56 nm and 58 nm, respectively. This trend can be explained by noting that changing the side group from an *m*-terphenyl group to triphenylbenzene broadened the distribution of electron density in the molecule as shown in Fig. 2; since electron transitions are available through HOMO and LUMO electron density distributions, such a broadening increased the number of such electronic transition channels and hence resulted in the increased FWHM value for **TPB-C-TPB**.¹¹ Type (B) molecules also showed a similar side group-dependent broadening effect of the electron distribution: the FWHM values of **DPA-C-DPA**, **DPA-C-TPA** and **TPA-C-TPA** were found to be 50 nm, 54 nm and 59 nm, respectively. In contrast to the solution state, high FWHM values were observed for **TP-C-TP** and **DPA-C-DPA** in the film state. The *m*-terphenyl and diphenylamine side groups are apparently not large enough to

completely eliminate intermolecular packing of chrysene core molecules in the film state.

To further understand how changing the side groups changed the properties of the compounds, time-dependent (TD)-DFT calculations were performed. The absorption and emission wavelengths as well as oscillator strengths of the molecules calculated using the TD-CAM-B3LYP/6-311G (d,p) level are presented in Table S2†. The trends of the calculated absorption and emission wavelengths of the compounds were similar to those derived experimentally. As shown in Table S2†, the HOMO→LUMO transitions of all compounds were calculated to be 60.5% or higher. This result indicates that HOMO→LUMO transition was the main electronic transition route, and that chrysene mainly distributed with electron density plays a key role in the electronic transition.

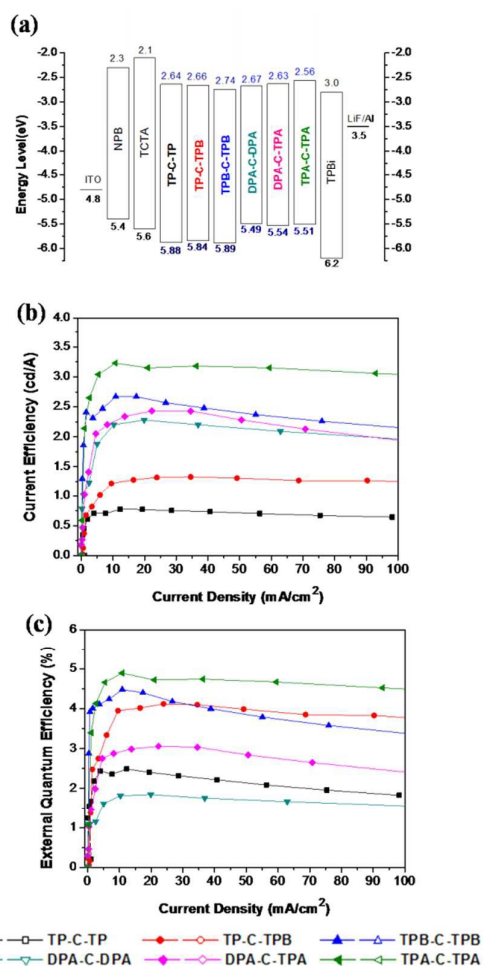
The absolute photoluminescence quantum efficiency (PLQY) values of the synthesized molecules were measured in the film state. Regarding the type (A) molecules, **TP-C-TP** yielded a PLQY value of 35%, while triphenylbenzene-containing **TP-C-TPB** and **TPB-C-TPB** showed higher values, of 53% and 48%. These results indicate that the side group apparently affected the molecular structure of the emission core.

Our group previously conducted a study on the anthracene core and reported that PL and electroluminescence (EL) efficiencies can be increased by substituting the *m*-terphenyl group (relative PLQY=0.1%) and triphenylbenzene (relative PLQY=0.17%) into the emission core, compared to substituting in the naphthalene side group, which yielded a relative PLQY of 0.08% (standard absolute PLQY: MADN).¹² Therefore, since substituting in a triphenylbenzene side group into the emission core yielded a higher relative quantum efficiency than did substituting in an *m*-terphenyl group, the PLQY and oscillator strength were increased as shown in Table 1 and Table S2†. Oscillator strength is closely associated with the electronic transition of molecule, and an increase of the oscillator strength indicates a contribution of greater energy to the electronic transition at the maximum absorption wavelength, hence increasing absorption and emission efficiencies.¹³ Consequently, PLQY values of triphenylbenzene-containing **TP-C-TPB** and **TPB-C-TPB** materials were greater than that of **TP-C-TP**.

Type (B) molecules also showed high PLQY values according to increased oscillator strength. Whereas **DPA-C-DPA** showed a quantum efficiency of 32%, the quantum efficiency of **DPA-C-TPA** was shown to be 64%. Most notably, **TPA-C-TPA** showed the greatest oscillator strength, at 1.27, and a high quantum efficiency of 70%. Of the six materials tested, **DPA-C-DPA** displayed the lowest quantum efficiency. Since diphenylamine is not a bulky side group, it was unable to effectively prevent packing of the chrysene core, which resulted in greater loss of energy from the excimer.

Table 2. Electroluminescence efficiency of synthesized compounds at 10 mA cm⁻².

Compound	Volt (v)	C.E. (cd/A)	P.E. (lm/W)	E.Q.E. (%)	CIE (x, y)	EL _{max} (nm)	EL FWHM (nm)
TP-C-TP	6.76	0.74	0.38	2.44	(0.158, 0.045)	422	64
TP-C-TPB	6.56	1.23	0.65	4.02	(0.154, 0.042)	431	60
TPB-C-TPB	6.87	2.62	1.31	4.41	(0.151, 0.075)	440	62
DPA-C-DPA	5.47	2.16	1.38	1.80	(0.174, 0.158)	454, 548	-
DPA-C-TPA	6.14	2.24	1.25	2.92	(0.147, 0.092)	451	51
TPA-C-TPA	5.47	3.19	2.03	4.83	(0.147, 0.077)	447	51

**Fig 4.** EL characteristics of devices using the synthetic materials as EMLs: (a) energy levels of organic materials, (b) luminance efficiency versus current density, (c) external quantum efficiency versus current density.

Electroluminescence Properties

Six different non-doped OLED devices (device configuration: ITO/N,N'-bis(naphthalen-1-yl)-N,N'-bis(phenyl)benzidine [NPB] 40 nm/tris(4-carbazoyl-9-ylphenyl)amine [TCTA] 20 nm / synthesized emitting materials 30 nm/1,3,5-tri(1-phenyl-1H-benzo[d]imidazol-2-yl)phenyl [TPBi] 20 nm/LiF 1nm/Al 200 nm) were prepared using the six synthesized molecules as the respective emitting layers (EMLs), and the EL performances of the devices were measured.

NPB was used as the hole-injection layer, and TCTA was used as hole-transporting and exciton-blocking layers. TPBi was used as electron-transporting and hole-blocking layers. Emitting materials were applied as a single layer with a non-doped structure.

For each of the six devices, the shape and maximum wavelength of the EL spectrum remained unchanged with an increase of current density from 10 mA cm⁻² to 100 mA cm⁻² (see Fig S8[†]). All of the devices were confirmed to properly form excitons in the EML and operate stably. The OLED device properties are summarized in Fig. 4 and Table 2.

TP-C-TP, with its bulky substituted side group, showed a current efficiency (C.E.) of 0.74 cd A⁻¹, power efficiency (P.E.) of 0.38 lm W⁻¹ and external quantum efficiency (EQE) of 2.44% at 10 mA cm⁻². It also showed excellent color coordinates of CIE x,y (0.158, 0.045). As chrysene, which has a large band gap, was combined with the *m*-terphenyl group, which reduces intermolecular interactions, ultra-deep-blue emission with a CIE y value of 0.048 was obtained from a non-doped OLED device.

Compared to **TP-C-TP**, **TP-C-TPB** showed an increased PLQY value with current and power efficiencies of 1.23 cd A⁻¹ and 0.65 lm W⁻¹, i.e., about 1.6 times higher than those of **TP-C-TP**, and with a high EQE of 4.01%. Notably, the FWHM of **TP-C-TPB** was observed to be only 60 nm, less than that of **TP-C-TP**, because intermolecular interactions were effectively suppressed by the introduction of bulky triphenylbenzene. As

a result, an ultra-deep-blue emission of CIE x,y (0.154, 0.042) was shown despite a slight reduction of its band gap and increase of its EL maximum by 9 nm. This emission simultaneously accomplished an EQE of over 4.0% and CIE y value below 0.05 in a non-doped device system, and is hence a world-class result, surpassing the CIE y maximum value of 0.06 for deep-blue color coordinates of the HDTV standard blue.

In the case of **TPB-C-TPB**, the band gap was reduced by the increase of the intramolecular conjugation length, and the maximum wavelength of the EL spectrum was red-shifted, to 440 nm, relative to the results for **TP-C-TP** and **TP-C-TPB**. The CIE y value was slightly increased to CIE x,y (0.151, 0.075). Despite this, the device showed excellent current and power efficiencies of 2.62 cd A^{-1} and 1.31 lm W^{-1} , and high EQE value of 4.41% because of the side group effect and improved PLQY value.

When type (B) materials, which contain aromatic amine side groups instead of bulky aromatic side groups, were applied as the EML, the devices were found to have relatively low turn-on voltages and operating voltages compared to the devices using type (A) molecules, thereby showing relatively high P.E. This difference resulted from the HOMO level being increased by the electron-donating amine moiety and the operating voltage being decreased by the lowered interface energy barrier.

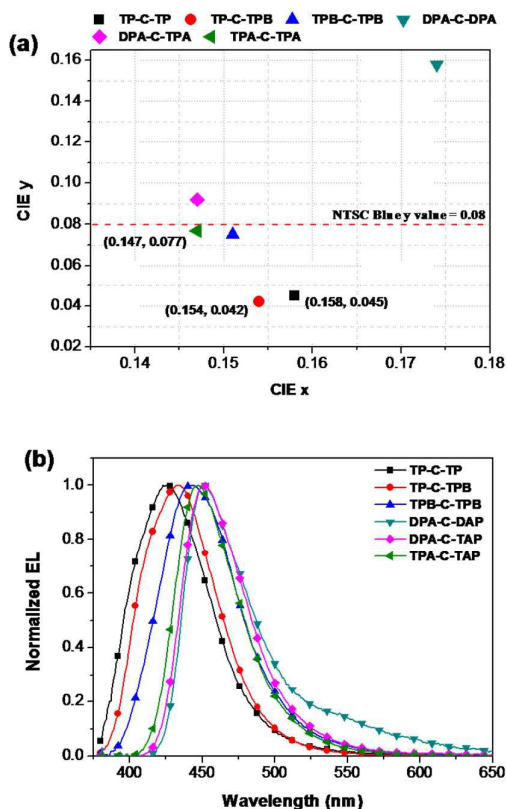


Fig 5. (a) CIE y values and (b) EL spectra of devices using synthesized compounds.

DPA-C-DPA showed current and power efficiencies of 2.16 cd A^{-1} and 1.38 lm W^{-1} . However, excimer formation by intermolecular packing resulted in a sky blue emission of CIE x,y (0.174, 0.158) and a low EQE of 1.80%. On the other hand, **DPA-C-TPA**, which has an asymmetric connection to the triphenylamine side group, was able to prevent excimers because of the bulkiness of this side group, and hence showed an increased current efficiency of 2.24 cd A^{-1} and EQE of 2.92% with a deep-blue emission of CIE x,y (0.147, 0.092).

Notably, **TPA-C-TPA** showed a high PLQY value (70%) and an EL spectrum having an extremely small FWHM of 51 nm due to the reduced intermolecular interactions. As a result, the current and power efficiencies were improved to 3.19 cd A^{-1} and 2.03 lm W^{-1} . An excellent deep-blue emission was achieved, with an EQE of 4.83% and CIE x,y of (0.147, 0.077) (See Fig 5).

Many existing studies of blue emitters based on anthracene and pyrene core chromophores introduced bulky side groups in the molecule, or created a highly twisted structure, for the purpose of suppressing molecular packing and reducing $\pi\text{-}\pi^*$ stacking to maintain a deep-blue emission.^{10, 14} These molecules could maintain the wavelength, but they experienced problems such as reduced efficiency and increased operating voltage due to extremely wide band gaps. There have been various attempts to achieve a low turn-on voltage through introduction of an electron-donating or electron-accepting moiety or a donor-acceptor type,¹⁵ but it was then extremely difficult to maintain the deep-blue emission since the band gap was reduced and the emission wavelength was red-shifted by intramolecular charge transfer. In this report, **TPA-C-TPA** synthesized using chrysene as the central core showed not only an increasing C.E. through high PLQY and increasing P.E. through decreasing operating voltage, but also better color coordinates than the NTSC blue (CIE y 0.08). This is an excellent result: deep-blue color coordinates were maintained and the P.E. increased 1.5 fold by controlling the electronic properties of the molecule, despite introduction of a side group with electron-donating and hole-transporting properties.

Experimental Section

General information

The $^1\text{H-NMR}$ spectra was recorded on Bruker Avance 300 spectrometers. The FAB+-mass and EI+-spectra were recorded on a JEOL, JMS-AX505WA, HP5890 series II. The optical absorption spectra were obtained by using a Lambda 1050 UV/Vis/NIR spectrometer (PerkinElmer). A PerkinElmer luminescence spectrometer LS50 (Xenon flash tube) was used to perform photoluminescence spectroscopy. The glass-transition temperatures (T_g) of the compounds were determined with differential scanning calorimetry (DSC) under a nitrogen atmosphere by using a DSC4000 (PerkinElmer). Samples were heated to $500 \text{ }^\circ\text{C}$ at a rate of $10 \text{ }^\circ\text{C min}^{-1}$ and cooled at $10 \text{ }^\circ\text{C min}^{-1}$ then heated again under the same heating conditions as used in the initial heating process.

Degradation temperatures (T_d) were determined with thermo gravimetric analysis (TGA) by using a TGA4000(PerkinElmer). Samples were heated to 700 °C at a rate of 10 °C min⁻¹. Time-resolved fluorescence lifetime and PL quantum yield were measured by an absolute PL quantum yield measurement system (QM-400 Spectrofluorometer). The HOMO energy levels were determined with ultraviolet photoelectron yield spectroscopy (Riken Keiki AC-2). The LUMO energy levels were derived from the HOMO energy levels and the band gaps. All DFT and TD-DFT calculations were performed using the Gaussian09¹⁶ program. In each of the EL devices, N,N'-bis(naphthalen-1-yl)-N,N'-bis(phenyl)benzidine (NPB) was used for the hole transporting and injection layer (HTL), tris(4-carbazoyl-9-ylphenyl)amine (TCTA) was used for the hole transporting and electron blocking layer, one of the synthetic materials **TP-C-TP**, **TP-C-TPB**, **TPB-C-TPB**, **DPA-C-DPA**, **DPA-C-TPA** and **TPA-C-TPA** was used as the emitting layer (EML), 1,3,5-tri(1-phenyl-1H-benzo[d]imidazol-2-yl)phenyl (TPBi) was used for the electron transporting and hole blocking layer (ETL), lithium fluoride (LiF) was used for the electron injection layer (EIL), and ITO was used as the anode and aluminum (Al) as the cathode. All organic layers were deposited under 10-6 Torr, with a rate of deposition of 1.0 Å s⁻¹ to create an emitting area of 4 mm². The LiF and aluminum layers were continuously deposited under the same vacuum conditions. The luminance efficiency data for the fabricated EL devices were obtained by using a Keithley 2400 electrometer. Light intensities were obtained with a Minolta CS-1000A. The operational stabilities of the devices were measured under encapsulation in a glove box.

Synthesis

Synthesis of 1-bromo-3,5-diphenylbenzene.[1]

1,3,5-tribromobenzene (20 g, 63 mmol), Pd(PPh₃)₄ (4.36g, 3.7 mmol) were added to 500 mL of dry THF solution. Then, phenylboronic acid (17g, 140 mmol) and 2M K₂CO₃ solution (50 mL), which was dissolved in H₂O, was added to the reaction mixture. The reaction mixture was heated to 65°C for 5h under nitrogen. After the reaction was finished, diethyl ether and water were extracted. The organic layer was dried with anhydrous MgSO₄ and filtered. The solvent was evaporated. The product was isolated by silica gel column chromatography using CHCl₃: hexane (1 : 15) eluent to afford a white solid. (Yield 61%) ¹H NMR (300MHz, CDCl₃, 25°C, TMS): δ=7.70(s, 3H), 7.60(d, 4H), 7.44(t, 4H), 7.36 ppm (t, 2H).

Synthesis of 1-borolane-3, 5-diphenylbenzene.[2]

Compound[1] (6.0g, 19.4 mmol) was dissolved in 400 mL of anhydrous THF solution and stirred at -78 °C. Then, the 2.0 M n-BuLi (10 mL) was added. Then, isopropoxy-4,4,5,5-tetramethyl-1,3,2-dioxaborolane (6 mL) was added to the reaction mixture. After the reaction was finished, diethyl ether and water were extracted. The organic layer was dried by evaporator. The product was recrystallized from chloroform and methanol. (Yield 86.9%) ¹H NMR (300MHz, CDCl₃, 25°C,

TMS): δ=8.03(s, 2H), 7.90(s, 1H), 7.69(d, 4H), 7.44(t, 4H), 7.35(t, 2H), 1.37 ppm (s, 12H).

Synthesis of 4-(4-bromophenyl)-2,6-diphenylbenzene. [3]

Compound [2] (2.5 g, 7.0 mmol), Pd(PPh₃)₄ (0.24g, 0.21 mmol) were added to 100 mL of dry THF solution. Then, 1,4-dibromobenzene (4.96g, 21 mmol) and 2M K₂CO₃ solution (3.5 mL), which was dissolved in H₂O, was added to the reaction mixture. The reaction mixture was heated to 65°C for 3h under nitrogen. After the reaction was finished, extracted with diethyl ether and water. The organic layer was dried with anhydrous MgSO₄ and filtered. The solvent was evaporated. The product was isolated by silica gel column chromatography using CHCl₃: hexane (1 : 10) eluent to afford a white solid. (Yield 77%) ¹H NMR (300MHz, CDCl₃, 25°C, TMS): δ=7.80(s, 1H), 7.74(s, 2H), 7.69(d, 4H), 7.58(m, 4H), 7.48(t, 4H), 7.39 ppm (t, 2H).

Synthesis of 4-(4-borolanophenyl)-2,6-diphenylbenzene.[4]

Compound[3] (4.0g, 10.3 mmol) was dissolved in 300 mL of anhydrous THF solution and stirred at -78°C. The 2.0 M n-BuLi (5.2 mL) was added. Then, isopropoxy-4,4,5,5-tetramethyl-1,3,2-dioxaborolane (3.06 mL) was added to the reaction mixture. After the reaction was finished, diethyl ether and water were extracted. The organic layer was dried by evaporator. The product was recrystallized from chloroform and methanol. (Yield 30.4%) ¹H NMR (300MHz, CDCl₃, 25°C, TMS): δ=7.93(s, 1H), 7.80(s, 2H), 7.71(d, 4H), 7.69(m, 4H), 7.39(t, 4H), 7.39(t, 2H) 1.35 ppm (s, 12H).

Synthesis of 4-(diphenylamino)phenylboronic acid.[5]

4-Bromo-triphenylamine (5 g, 15.4 mmol) was added in 200 mL of dry THF solution and stirred at -78 °C, then 2.0 M n-BuLi (7.7 mL) was added. Next, triethyl borate (3.93 mL) was added to the reaction mixture after 30 min. After the reaction had finished, HCl 35wt% solution was added to the reaction mixture after 3h. The reaction mixture was extracted with diethyl ether and water. The organic layer was dried with anhydrous MgSO₄ and filtered. The mixture was evaporated. The product was recrystallized from dichloromethane (CH₂Cl₂) and hexane. (Yield 65%). ¹H NMR (300MHz, CDCl₃, 25°C, TMS): δ=8.77 (m, 2H), 8.63 (d, 1H), 7.62 (m, 3H), 7.35 (t, 2H), 7.22 ppm (m, 4H).

Synthesis of 6,12-bis(3',5'-diphenylphenyl)chrysene, TP-C-TP [6]

Compound [2] (1.38 g, 3.90 mmol), Pd(PPh₃)₄ (0.09g, 0.08 mmol) were added to 150 mL of dry toluene solution. Then, 6,12-dibromo-chrysene (0.5g, 1.3 mmol) and 2M K₂CO₃ solution (15 mL), which was dissolved in H₂O, was added to the reaction mixture. The reaction mixture was heated to 110°C for 8h under nitrogen. After the reaction was finished, chloroform and water were extracted. The organic layer was dried with anhydrous MgSO₄ and filtered. The solvent was evaporated. The product was isolated by silica gel column chromatography using CHCl₃: hexane (1 : 1). The product was recrystallized from chloroform and methanol. (Yield 53%) ¹H

NMR (300MHz, [D₈]THF, 25°C, TMS): δ=9.07 (d, 2H), 8.95 (s, 2H), 8.19 (d, 2H), 8.15 (s, 2H), 7.94 (s, 4H), 7.83 (d, 8H), 7.70 (t, 2H), 7.59 (t, 2H), 7.47 (t, 8H), 7.36 ppm (t, 4H). EI⁺-Mass: 684, Anal. calcd for C₅₄H₃₆: C 94.7, H 5.30; found: C 94.89, H 5.12%.

Synthesis of 6-Bromo-12-[1,1';3',1'']terphenyl-5'-yl-chrysene [7]

Compound [2] (0.69 g, 1.8 mmol), Pd(PPh₃)₄ (0.07g, 0.07 mmol) were added to 200 mL of dry toluene solution. Then, 6,12-dibromo-chrysene (0.5g, 1.3 mmol) and 2M K₂CO₃ solution (8 mL), which was dissolved in H₂O, was added to the reaction mixture. The reaction mixture was heated to 80°C for 6h under nitrogen. After the reaction was finished, chloroform and water were extracted. The organic layer was dried with anhydrous MgSO₄ and filtered. The solvent was evaporated. The product was isolated by silica gel column chromatography using CHCl₃: hexane (1 : 4) eluent to afford a white solid. (Yield 57%) ¹H NMR (300MHz, [D₈]THF, 25°C, TMS): δ=9.26 (s, 1H), 9.01 (m, 2H), 8.87 (s, 1H), 8.45 (m, 1H), 8.16 (d, 1H), 8.05 (s, 1H), 7.90 (s, 2H), 7.82 (d, 4H), 7.76 (m, 3H), 7.76 (t, 1H), 7.45 (t, 4H), 7.36 ppm (t, 2H).

Synthesis of 6-(3',5'-diphenylphenyl)-12-(3''',5''-diphenyl biphenyl -4''-yl)chrysene, TP-C-TPB [8]

Compound[7] (0.5 g, 0.93 mmol), Pd(PPh₃)₄ (0.11g, 0.09 mmol) were added to 150 mL of dry toluene solution. Then, compound[4] (0.6g, 1.4 mmol) and 2M K₂CO₃ solution (7.5 mL), which was dissolved in H₂O, was added to the reaction mixture. The reaction mixture was heated to 110°C for 5h under nitrogen. After the reaction was finished, chloroform and water were extracted. The organic layer was dried with anhydrous MgSO₄ and filtered. The solvent was evaporated. The product was isolated by silica gel column chromatography using CHCl₃: hexane (1 : 4) eluent to afford a white solid. (Yield 65%) ¹H NMR (300MHz, [D₈]THF, 25°C, TMS): δ=9.04 (t, 2H), 8.94 (s, 1H), 8.87 (s, 1H), 8.19 (d, 1H), 8.14 (d, 1H), 8.03 (m, 5H), 8.79 (m, 3H), 7.89 (m, 10H), 7.73 (m, 2H), 7.60 (t, 2H), 7.47 (m, 8H), 7.38 ppm (m, 4H). EI⁺-Mass: 760, Anal. calcd for C₆₀H₄₀: C 94.7, H 5.30; found: C 94.62, H 5.33%.

Synthesis of 6,12-bis(3'',5''-diphenylbiphenyl-4''-yl)chrysene, TPB-C-TPB [9]

Compound [4] (1.68 g, 3.9 mmol), Pd(PPh₃)₄ (0.09g, 0.08 mmol) were added to 200 mL of dry toluene solution. Then, 6,12-dibromo-chrysene (0.5g, 1.3 mmol) and 2M K₂CO₃ solution (10 mL), which was dissolved in H₂O, was added to the reaction mixture. The reaction mixture was heated to 110°C for 8h under nitrogen. After the reaction was finished, chloroform and water were extracted. The organic layer was dried with anhydrous MgSO₄ and filtered. The solvent was evaporated. The product was isolated by silica gel column chromatography using CHCl₃: hexane (1 : 2) eluent to afford a white solid. (Yield 55%) ¹H NMR (300MHz, [D₆]DMSO, 25°C, TMS): δ=9.13 (d, 2H), 8.89 (s, 2H), 8.16 (d, 4H), 8.06 (m, 6H), 7.95 (m, 10H), 7.82 (m, 6H), 7.75 (t, 2H), 7.55 (t, 8H), 7.45 ppm (t, 4H). EI⁺-Mass: 836, Anal. calcd for C₆₆H₄₄: C 94.7, H 5.30; found: C 94.61, H 5.37%.

Synthesis of N,N,N',N'-tetraphenyl-chrysene-6,12-diamine, DPA-C-DPA [10]

Diphenyl-amine (0.66 g, 3.91 mmol), Pd2(dba)₃ (0.18g, 0.19 mmol), sodium tetra butoxide (0.63 g, 6.5 mmol) were added to 200 mL of dry toluene solution. Then, 6,12-dibromo-chrysene (0.5g, 1.3 mmol) and tri-tert-butylphosphine solution (0.2 mL), which was dissolved in toluene, was added to the reaction mixture. The reaction mixture was heated to 100°C for 10h under nitrogen. After the reaction was finished, diethyl ether and water were extracted. The organic layer was dried with anhydrous MgSO₄ and filtered. The solvent was evaporated. The product was isolated by silica gel column chromatography using CHCl₃: hexane (1 : 3) eluent to afford a white solid. (Yield 48%) ¹H NMR (300MHz, [D₈]THF, 25°C, TMS): δ=8.76 (s, 2H), 8.62 (d, 2H), 8.12 (d, 2H), 7.57 (t, 2H), 7.45 (t, 2H), 7.19 (t, 8H), 7.14 (d, 8H), 6.92 ppm (t, 4H). EI⁺-Mass: 562, Anal. calcd for C₄₂H₃₀N₂: C 89.65, H 5.37, N 4.98; found: C 89.84, H 5.18, N 4.97%.

Synthesis of [4-(12-Bromo-chrysen-6-yl)-phenyl]-diphenyl-amine, [11]

Compound [5] (0.45 g, 1.56 mmol), Pd(PPh₃)₄ (0.15g, 0.13 mmol) were added to 100 mL of dry toluene solution. Then, 6,12-dibromo-chrysene (0.5g, 1.3 mmol) and 2M K₂CO₃ solution (10 mL), which was dissolved in H₂O, was added to the reaction mixture. The reaction mixture was heated to 110°C for 4h under nitrogen. After the reaction was finished, diethyl ether and water were extracted. The organic layer was dried with anhydrous MgSO₄ and filtered. The solvent was evaporated. The product was isolated by silica gel column chromatography using CHCl₃: hexane (1 : 2) eluent to afford a white solid. (Yield 42%) ¹H NMR (300MHz, [D₈]THF, 25°C, TMS): δ=9.22 (s, 1H), 8.93 (m, 2H), 8.73 (s, 1H), 8.41 (m, 1H), 8.12 (d, 1H), 7.76 (m, 3H), 7.64 (t, 1H), 7.52 (d, 2H), 7.33 (m, 10H), 7.04 ppm (t, 2H).

Synthesis of [12-(4-diphenylamino-phenyl)-chrysen-6-yl]-diphenylamine, DPA-C-TPA [12]

Diphenyl-amine (0.23 g, 1.3 mmol), Pd2(dba)₃ (0.35g, 0.13 mmol), sodium tetra butoxide (0.75g, 7.8 mmol) were added to 150 mL of dry toluene solution. Then, compound[11] (0.5g, 0.91 mmol) and tri-tert-butylphosphine (0.2 mL), which was dissolved in toluene, was added to the reaction mixture. The reaction mixture was heated to 85°C for 12h under nitrogen. After the reaction was finished, diethyl ether and water were extracted. The organic layer was dried with anhydrous MgSO₄ and filtered. The solvent was evaporated. The product was isolated by silica gel column chromatography using CHCl₃: hexane (1 : 3) eluent to afford a white solid. (Yield 68%). ¹H NMR (300MHz, [D₈]THF 25°C, TMS): δ=8.95 (d, 1H), 8.75 (s, 1H), 8.69 (s, 1H), 8.63 (d, 1H), 8.12 (t, 2H), 7.63 (m, 6H), 7.30 (m, 5H), 7.14 (m, 13H), 7.04 (t, 2H), 6.91 ppm (t, 2H). EI⁺-Mass: 638, Anal. calcd for C₄₈H₃₄N₂: C 90.25, H 5.36, N 4.39; found: C 89.91, H 5.32, N 4.45%.

Synthesis of 6,12-bis[4-(diphenylamino)phenyl]chrysene, TPA-C-TPA [13]

Compound [5] (1.13 g, 3.9 mmol), Pd(PPh₃)₄ (0.12g, 0.11 mmol) were added to 200 mL of dry toluene solution. Then, 6,12-dibromo-chrysene (0.5g, 1.3 mmol) and 2M K₂CO₃ solution (10 mL), which was dissolved in H₂O, was added to the reaction mixture. The reaction mixture was heated to 110°C for 7h under nitrogen. After the reaction was finished, diethyl ether and water were extracted. The organic layer was dried with anhydrous MgSO₄ and filtered. The solvent was evaporated. The product was isolated by silica gel column chromatography using CHCl₃: hexane (1 : 2) eluent to afford a white solid. (Yield 56%) ¹H NMR (300MHz, [D₈]THF 25°C, TMS): δ=9.00 (d, 2H), 8.77 (s, 2H), 8.13 (d, 2H), 7.69 (t, 2H), 7.54 (m, 6H), 7.30 (m, 10H), 7.21 (m, 10H), 7.04 ppm (t, 4H). EI⁺-Mass: 714, Anal. calcd for C₈₄H₃₈N₂: C 90.72, H 5.36, N 3.92; found: C 90.67, H 5.33, N 3.97%.

Conclusions

The chrysene group, with its large band gap, was selected as a central core structure for designing new molecules that emit ultra-deep-blue light with high efficiency. The effects of different side groups on the intrinsic properties of the chrysene core were systematically investigated. As a result, the oscillator strength of the chrysene core molecule was increased by selecting an appropriate side group, and an improved PLQY value was obtained. Also, the substitution of electron-donating side groups into the chrysene core was shown to affect the optical and physical properties of the molecule. The synthesized materials were applied as EMLs in non-doped devices, and the **TP-C-TPB** device afforded efficient ultra-deep-blue emission below the HDTV standard blue (CIE y 0.06), with an EQE of 4.02% and excellent color coordinates of CIE x,y (0.151, 0.042). In addition, **TPA-C-TPA**, which introduced triphenylamine with hole-transporting properties, exhibited a low operating voltage and an excellent EQE of 4.83%, while showing color coordinates of CIE x,y (0.147, 0.077), below NTSC blue (CIE y 0.08). Such results for molecules based on the chrysene core with its large band gap are expected to help the development of materials that can maintain a highly efficient emission of deep-blue light. The conclusions section should come in this section at the end of the article, before the acknowledgements.

Acknowledgements

Development Program for Strategic Core Materials funded by the Ministry of Trade, Industry & Energy, Republic of Korea (Project No. 10047758).

Notes and references

- (a) C. W. Tang and S. A. Van Slyke, *Appl. Phys. Lett.*, 1987, **51**, 913; (b) Y. R. Sun, N. Giebink, C. Kanno, B. Ma, M. E. Thompson and S. R. Forrest, *Nature.*, 2006, **440**, 908; (c) M. F. Wu, S. J. Yeh, C. T. Chen, H. Murayama, T. Tsuboi, W. S. Li,

- I. Chao, S. W. Liu and J. K. Wang, *Adv. Funct. Mater.*, 2007, **17**, 1887; (d) Z. Zhao, C. Deng, S. Chen, J. W. Y. Lam, W. Qin, P. Lu, Z. Wang, H. S. Kwok, Y. Ma, H. Qiu and B. Z. Tang, *Chem. Commun.*, 2011, **47**, 8847; (e) H. Wu, G. Zhou, J. Zou, C. L. Ho, W. Y. Wong, W. Yang, J. Peng and Y. Cao, *Adv. Mater.*, 2009, **21**, 4181; (f) M. C. Gather, A. Kohnen, A. Falcou, H. Becker and K. Meerholz, *Adv. Funct. Mater.*, 2007, **17**, 191; (g) J. Huang, X. Wang, A. J. deMello, J. C. deMello and D. D. C. Bradley, *J. Mater. Chem.*, 2007, **17**, 3551; (h) B. Chen, J. Ding, L. Wang, X. Jing and F. Wang, *Chem. Commun.*, 2012, **48**, 8970; (i) M. Yu, S. Wang, S. Shao, J. Ding, L. Wang, X. Jing and F. Wang, *J. Mater. Chem. C*, 2015, **3**, 861; (j) L. Zhao, S. Wang, S. Shao, J. Ding, L. Wang, X. Jing and F. Wang, *J. Mater. Chem. C*, 2015, **3**, 8859.
- (a) R. Capelli, S. Toffanin, G. Generali, H. Usta, A. Facchetti, M. Muccini, *Nature Materials.*, 2010, **9**, 496; (b) Y. Yang, R. T. Farley, T. T. Steckler, S. H. Eom, J. R. Reynolds, K. S. Schanze, J. Xue, *J. Appl. Phys.*, 2009, **106**, 044509; (c) T. Tsuzuki, S. Tokito, *Adv. Mater.*, 2007, **19**, 276; (d) B. R. Lee, W. Lee, T. L. Nguyen, J. S. Park, J. S. Kim, J. Y. Kim, H. Y. Woo, M. H. Song, *Appl. Mater. Interfaces.*, 2013, **5**, 5690; (e) M. Cocchi, D. Virgili, V. Fattori, D. L. Rochester, J. A. G. Williams, *Adv. Funct. Mater.*, 2007, **17**, 285; (f) Y. Liu, S. Chen, J. W. Y. Lam, P. Lu, R. T. K. Kwok, F. Mahtab, H. S. Kwok, B. Z. Tang, *Chem. Mater.*, 2011, **23**, 2536; (g) J. You, S. L. Lai, W. Liu, T. W. Ng, P. Wang, C. S. Lee, *J. Mater. Chem.*, 2012, **22**, 8922; (h) J. K. Bin, J. I. Hong, *Org. Electron.*, 2012, **13**, 2893; (i) M. M. Rothmann, S. Haneder, E. D. Como, C. Lennartz, C. Schildknecht, P. Strohriegel, *Chem. Mater.*, 2010, **22**, 2403; (j) Y. I. Park, J. H. Son, J. S. Kang, S. K. Kim, J. H. Lee, J. W. Park, *Chem. Commun.*, 2008, 2143; (k) J. H. Ahn, C. Wang, I. F. Perepichka, M. R. Bryce, M. C. Petty, *J. Mater. Chem.*, 2007, **17**, 2996.
- J. -Y. Hu, Y. -J. Pu, F. Satoh, S. Kawata, H. Katagiri, H. Sasabe, J. Kido, *Adv. Funct. Mater.*, 2014, **24**, 2064.
- (a) N. C. Giebink, B. W. D'Andrade, M. S. Weaver, P. B. Mackenzie, J. J. Brown, M. E. Thompson, S. R. Forrest, *J. Appl. Phys.*, 2008, **103**, 44509; (b) I. R. de Moraes, S. Scholz, B. Lussem, K. Leo, *Org. Electron.*, 2011, **12**, 341.
- (a) D. Bailey, V. E. Williams, *Chem. Commun.*, 2005, 2569; (b) C. -H. Chien, C. -K. Chen, F. -M. Hsu, C. -F. Shu, P. -T. Chou, C. -H. Lai, *Adv. Funct. Mater.*, 2009, **19**, 560; (c) S. -H. Lin, F. -I. Wu, R. -S. Liu, *Chem. Commun.*, 2009, 6961; (d) K. Danel, T. -H. Huang, J. T. Lin, Y. -T. Tao, C. -H. Chuen, *Chem. Mater.*, 2002, **14**, 3860.
- (a) S. L. Lai, Q. X. Tong, M. Y. Chan, T. W. Ng, M. F. Lo, S. T. Lee, C. S. Lee, *J. Mater. Chem.*, 2011, **21**, 1206; (b) T. M. Figueira-Duarte, P. G. D. Rosso, R. Trättnig, S. Sax, E. J. W. List, K. Mullen, *Adv. Mater.*, 2010, **22**, 990; (c) K.-C. Wu, P.-J. Ku, C.-S. Lin, H.-T. Shih, F.-I. Wu, M.-J. Huang, J.-J. Lin, I.-C. Chen, C.-H. Cheng, *Adv. Funct. Mater.*, 2008, **18**, 67; (d) M. Y. Lo, C. Zhen, M. Lauters, G. E. Jabbour, A. Sellinger, *J. Am. Chem. Soc.*, 2007, **129**, 5808; (e) K. R. Justin Thomas, N. Kapoor, M. N. K. Prasad Bolisetty, J.-H. Jou, Y.-L. Chen, Y.-C. Jou, *J. Org. Chem.*, 2012, **77**, 3921.
- (a) E. J. W. List, R. Guentner, P. Scanducci de Freitas, U. Scherf, *Adv. Mater.*, 2002, **14**, 374; (b) J. U. Wallace, S. H. Chen, *Adv. Polym. Sci.*, 2008, **12**, 152; (c) Y. Zhang, G. Cheng, Y. Zhao, J. Y. Hou, S. Y. Liu, S. Tang, Y. G. Ma, *Appl. Phys. Lett.*, 2005, **87**, 241112; (d) S. Tang, M. Liu, P. Lu, G. Cheng, M. Zeng, Z. Q. Xie, H. Xu, H. P. Wang, B. Yang, Y. G. Ma, D. H. Yan, *Org. Electron.*, 2008, **9**, 241; (e) S. O. Jeon, Y. M. Jeon, J. W. Kim, C. W. Lee, M. S. Gong, *Org. Electron.*, 2008, **9**, 522; (f) C.-C. Wu, Y.-T. Lin, K.-T. Wong, R.-T. Chen, Y.-Y. Chien, *Adv. Mater.*, 2004, **16**, 61; (g) K.-T. Wong, R.-T. Chen, F.-C. Fang, C.-C. Wu, Y.-T. Lin, *Org. Lett.*, 2005, **7**, 1979; (h) C. -G. Zhen, Y. -F. Dai, W. -J. Zeng, Z. Ma, Z. -K. Chen, J. Kieffer, *Adv. Funct. Mater.*, 2011, **21**, 699.

- 8 Y. Park, S. Kim, J.-H. Lee, D. H. Jung, C. -C. Wu, J. Park, *Org. Electron.*, 2010, **11**, 864.
- 9 Y. Park, B. Kim, C. Lee, A. Hyun, S. Jang, J. H. Lee, Y. S. Gal, T. H. Kim, K. S. Kim, J. Park, *J. Phys. Chem. C.*, 2011, **115**, 4843.
- 10 (a) S. Tao, Y. Jiang, S. -L. Lai, M. -K. Fung, Y. Zhou, X. Zhang, W. Zhao, C. -S. Lee, *Org. Electron.*, 2011, **12**, 358; (b) S. L. Lai, Q. X. Tong, M. Y. Chan, T.W. Ng, M. F. Lo, C. C. Ko, S. T. Lee, C. S. Lee, *Org. Electron.*, 2011, **12**, 541; (c) C. -L. Wu, C. -H. Chang, Y. -T. Chang, C. -Ti. Chen, C. -T. Chen, C. -J. Su, *J. Mater. Chem. C.*, 2014, **2**, 7188.
- 11 Y. Park, J. -H. Lee, D. H. Jung, S. -H. Liu, Y. -H. Lin, L. -Y. Chen, C. -C. Wud, J. Park, *J. Mater. Chem.*, 2010, **20**, 5930.
- 12 (a) S. -K. Kim, B. Yang, Y. Park, Y. Ma, J. -Y. Lee, H. -J. Kim, J. Park, *Org. Electron.*, 2009, **10**, 822; (b) S. -K. Kim, B. Yang, Y. Ma, J. -H. Lee, J. Park, *J. Mater. Chem.*, 2008, **18**, 3376; (c) H. Lee, B. Kim, S. Kim, J. Kim, J. Lee, H. Shin, J. -H. Lee, J. Park, *J. Mater. Chem. C.*, 2014, **2**, 4737.
- 13 (a) K. Sumi, Y. Niko, K. Tokumaruz, G. Konishi, *Chem. Commun.*, 2013, **49**, 3893; (b) Z. Gao, Z. Wang, T. Shan, Y. Liu, F. Shen, Y. Pan, H. Zhang, X. He, P. Lu, B. Yang, Y. Ma, *Org. Electron.*, 2014, **15**, 2667; (c) Q. Zhang, H. Kuwabara, W. J. Potscavage, Jr, S. Huang, Y. Hatae, T. Shibata, C. Adachi, *J. Am. Chem. Soc.*, 2014, **136**, 18070.
- 14 (a) Y. -H. Yua, C. -H. Huang, J. -M. Yeh, P. -T. Huang, *Org. Electron.*, 2011, **12**, 694; (b) S. Ye, J. Chen, C. Di, Y. Liu, K. Lu, W. Wu, C. Du, Y. Liu, Z. Shuai, G. Yu, *J. Mater. Chem.*, 2010, **20**, 3186; (c) Y. -Y. Lyu, J. Kwak, O. Kwon, S. -H. Lee, D. Kim, C. Lee, K. Char, *Adv. Mater.*, 2008, **20**, 2720; (d) S. L. Lin, L. H. Chan, R. H. Lee, M. Y. Yen, W. J. Kuo, C. T. Chen, R. J. Jeng, *Adv. Mater.*, 2008, **20**, 3947; (e) Y. Zou, J. Zou, T. Ye, H. Li, C. Yang, H. Wu, D. Ma, J. Qin, Y. Cao, *Adv. Funct. Mater.*, 2011, **23**, 1781.
- 15 (a) Q. Zhang, J. Li, K. Shizu, S. H, S. Hirata, H. Miyazaki, C. Adachi, *J. Am. Chem. Soc.*, 2012, **134**, 14706; (b) W. Li, D. Liu, F. Shen, D. Ma, Z. Wang, T. Feng, Y. Xu, B. Yang, Y. Ma, *Adv. Funct. Mater.*, 2012, **22**, 2797; (c) K. H. Lee, L. K. Kang, J. Y. Lee, S. Kang, S. O. Jeon, K. S. Yook, J. Y. Lee, S. S. Yoon, *Adv. Funct. Mater.*, 2012, **20**, 1345; (d) L. Shi, Zhi. Liu, G. Dong, L. Duan, Y. Qiu, J. Jia, W. Guo, D. Zhao, D. Cui, X. Tao, *Chem. Eur. J.*, 2012, **18**, 8092.
- 16 M. J. Frisch, G. W. Trucks, H. B. Schlegel, G. E. Scuseria, M. A. Robb, J. R. Cheeseman, G. Scalmani, V. Barone, B. Mennucci, G. A. Petersson, H. Nakatsuji, M. Caricato, X. Li, H. P. Hratchian, A. F. Izmaylov, J. Bloino, G. Zheng, J. L. Sonnenberg, M. Hada, M. Ehara, K. Toyota, R. Fukuda, M. I. J. Hasegawa, T. Nakajima, Y. Honda, O. Kitao, H. Nakai, T. Vreven, J. A. Montgomery, Jr., J. E. Peralta, F. Ogliaro, M. Bearpark, J. J. Heyd, E. Brothers, K. N. Kudin, V. N. Staroverov, R. Kobayashi, J. Normand, K. Raghavachari, A. Rendell, J. C. Burant, S. S. Iyengar, J. Tomasi, M. Cossi, N. Rega, J. M. Millam, M. Klene, J. E. Knox, J. B. Cross, V. Bakken, C. Adamo, J. Jaramillo, R. Gomperts, R. E. Stratmann, O. Yazyev, A. J. Austin, R. Cammi, C. Pomelli, J. W. Ochterski, R. L. Martin, K. Morokuma, V. G. Zakrzewski, G. A. Voth, P. Salvador, J. J. Dannenberg, S. Dapprich, A. D. Daniels, © Farkas, J. B. Foresman, J. V. Ortiz, J. Cioslowski, D. J. Fox, Gaussian, Inc., Wallingford CT 2009.



Journal Name

ARTICLE

Highly Efficient Emitters of Ultra-Deep-Blue Light Made from Chrysene Chromophores

Hwangyu Shin, Hyecheol Jung, Beomjin Kim, Jaehyun Lee, Jiwon Moon, Joonghan Kim, and Jongwook Park *

The chrysene group, with its large band gap and high stability, was selected as a central core structure for designing new molecules that emit ultra-deep-blue light with high efficiency. Use of synthesized materials in a non-doped OLED device resulted in ultra-deep-blue emission with CIE x,y (0.154, 0.042) and CIE x,y (0.147, 0.077).

